Kinetics and Thermal Crystallinity of Recycled PET. I. Dynamic Cooling Crystallization Studies on Blends Recycled with Engineering PET

DAW-MING FANN, STEVE K. HUANG, and JIUNN-YIH LEE*

Graduate School of Textile and Polymer Engineering, National Taiwan Institute of Technology, Taiwan, Republic of China

SYNOPSIS

The recycled poly(ethylene terephthalate) (R-PET) from the recovery of a blow-molded bottle is studied with its crystalline behavior in terms of glass transition temperature (T_g), crystallization temperature (T_c), melting temperature (T_m), and its dynamic crystallization kinetics. These crystalline behaviors offer an explanation of the better mechanical properties of the R-PET. Thermal cycles of the processes of the R-PET and its blending specimens with engineering PET (E-PET) show the importance of the thermal treatment of the plastic PET in the improvements of mechanical strength and increased crystallinity. Tenfold and fivefold increases, respectively, of elongation and impact strength are observed in the specimen of R-/E-PET of 20/80 weight ratio blend, better than that of E-PET alone. A nearly 20-fold increase of the crystallization rate constant (K) at 190°C for the same R-/E-20/80 blend is observed. The Avrami exponent ("n") is found to be variable with temperature. The changing crystallization mechanisms are mainly the result of the competition between the nucleating and growing of crystallites in response to the temperature-controlling factor at the melt state. © 1996 John Wiley & Sons, Inc.

INTRODUCTION

One of the primary factors affecting the mechanical properties of semicrystalline poly(ethylene terephthalate) (PET) polymers is related to its crystalline and amorphous regions in the morphological structures. Recent reports on the crystallization kinetics of the PET are focused on engineering grade and not on the recycled PET materials. Cobbs and Burton[1] used infrared and density methods to study the crystallization kinetics on the PET film, while Morgan and colleagues[2,3] studied PET with various molecular weights and by density gradient and balance methods. They indicated that the fusion state of the sample is important for the consistent behavior of the crystallization and found that the crystallization rates were affected by the molecular weights. Other studies found a catalytic residual effect on the crystallization rates (Jackson and Longman[4]). A direct observation method of scattering angles and intensity has been reported by Van Antwerpen and Van Krevelen[5] and observation with a real-time small-angle light scattering on the rates was reported by Tant and Culberson[6] that indicated that the spherulite growth rate is inversely proportional to the molecular weight and is found to be in accordance with the Hoffman equation.[7] Tant and Culberson also obtained the identical temperature of the maximum crystallization rate that occurred on either the melt or the glassy states of the samples. By contrast, the finding that the temperature of the maximum crystallization rate occurred differently than that of either the melt or the glassy state was also reported (Bararnov et al.[8]). Taking consideration of various factors of the differential scanning calorimeter (DSC) study, the PET rates of crystallizations with isothermal and dynamic methods were also reported (Jabarin[9,10]) with the consistent results of both methods. With this indication, the dynamic

* To whom correspondence should be addressed.

Journal of Applied Polymer Science, Vol. 61, 1375–1385 (1996)
 CCC 0021-8995/96/081375-11

Table I Process Condition of Injection Molding

Sample Drying (°C)	120
Drying (h)	2
Cylinder setting temp. (°C)	270–280
Mold control temp. (°C)	30–40
Injection-maintain pressure	
Gauge (kg/cm^2)	40–60
Back (kg/cm^2)	40
Time (s)	30
Product cooling time (s)	60–80
Nozzle type	open
Screw diameter (m/m)	30

Conditions may vary at different machines.

crystallization method, which more closely simulates the fabrication process, is adapted for our study on the crystallinity of the recycled PET (R-PET).

In our previous studies, the reclamation of R-PET and blends with virgin PET for acceptable end products of injection and fiber fabrication are reported.[11,12] In this article, it is our intent to study the effects of the recycling process on the crystalline behavior of the R-PET and on its mechanical properties. Taking into consideration the recycling of the PET, reuses of the R-PET in blending with E-PET, and subjecting it to the various processing conditions of injection molding, samples of R-/E-PET blends are prepared. Samples subjected to various conditions such as being flaked, chipped, and injection molded at different recovery stages are included.

EXPERIMENTAL

Materials

Recovered PET materials were the irregular beverage bottle products selected from the production line, which were then crushed to flakes. Virgin PET resins were engineering injection grade. Both recovered PET and engineering-grade PET are a gift of Shin Kong Synthetic Fibers Corp., Taiwan. A fairly detailed characterization of the polymers and blends are listed in part II of this series [see *J. Appl. Polym. Sci.*, **61,** 261 (1996)], including the measurements of end groups and the molecular weights. The materials and nomenclature used for this study are as follows: VB, virgin blowing-grade resin; B-PET, injection-molded VB resin; flake, bottle crushed to flake; chip, flake extruded to chip; R-PET, injection molded with recycled chip; R80/E20, R50/E50, and R20/E80, injection-molded blends of recycled chip and engineering PET; E-PET, injection-molded engineering PET.

General Procedures of Processing

General procedures as shown below were followed to obtain various ratios of blends of injection-molding products: bottles → crush to flake → preheating dehydration → extrusion pelletized → pellets dry blend → preheating dehydration → melt/blended → injection → cooling → demolding. Pelletization was performed with a twin-screw extruder with a heating zone set between 250 and 260°C. The conditions of injection molding are shown in Table I.

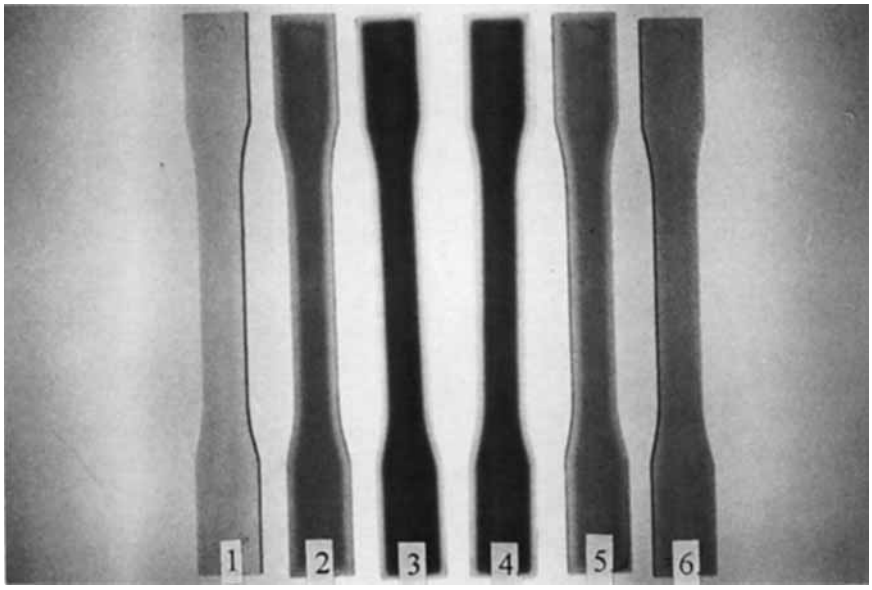

Figure 1 Injection-molding products of PET and R-PET blends. (1) B-PET, (2) R-PET, (3) R80/E20, (4) R50/E50, (5) R20/E80, (6) E-PET.

Table II Mechanical Properties of R-/E-PET Blend

Property	E-PET R-PET	100 0	80 20	50 50	20 80	0 100
Tensile (kg/cm^2)		653	672	653	623	
Elongation (%)		20	264	187	190	295
Impact (kg-cm/cm)		1.10	4.97	3.58	3.32	3.70

Testing of the Mechanical Properties

Tensile strengths were measured according to ASTM D638. The impact strengths were tested by ASTM D256.

Measurements with the DSC

Dynamic Crystallization with Cooling Mode

The samples were heated at a rate of 10°C/min up to 294°C and then held at that temperature for 15 min, for the start. The dynamic crystallization condition was monitored by using programmed cooling of the sample covering the range of 5–40°C/min[10] with Perkin Elmer DSC-7. The calorimeter is used for the measurements of the rate of the evolution of heat, and the area under the exotherm is related to the heat of crystallization.

The Avrami equation has been used to describe the nonisothermal crystallization and has been extended by Ozawa.[13] The modified Avrami equation is used in this study and is given by

$$1 - a(T) = e^{-K(T)/R^n} \quad (1)$$

where term $a(T)$ is the amount of transformed material at temperature T, $K(T)$ is the rate, R is the cooling rate, and n is the Avrami exponent. Equation (1) can be represented as

$$\log[-\ln(1 - a)] = \log K - n \log R \quad (2)$$

A plot of $\log[-\ln(1 - a)]$ against $\log R$ at a given temperature yields a straight line with a slope of $(-n)$ and the intercept of $\log K$.

DSC Thermogram Study

The DSC runs were made at heating rate of 10°C/min with the temperature range of 40–294°C. The recorded thermograms are used for the calculations of all of the first-order and second-order transitions, including glass transitions, crystallization, and fusion. Definition of the following terms follows the ASTM D3418, with T_c for crystallization peak temperature, T_m for melting peak temperature, and T_g for glass transition (midpoint) temperature.

RESULTS AND DISCUSSION

Characteristics of R-PET and Blended with E-PET

PET beverage bottles are made by the blow-molding process, which requires rather pure and slow-crystallized PET materials. The recycled, or accurately, the recovered PET (R-PET) was bottle selected from the production line, uncontaminated, and was subjected to series of thermal treatments of crushing, repelletting, injection molding, and so forth. The injection-molding process can be important for the reuses of the R-PET, such as with the blending of E-PET in the process. Some of the injection-molded samples of the R-PET, E-PET, and the blends of R-/E-PETs are shown in Figure 1. Opacity of the blends rather than the clarity of either unblended R-PETs or E-PETs is observed and can be attributed to different degrees of crystallinity since turbidity is often an index of crystallinity in PET materials. For comparison, the most clear sample was injection molded with virgin blowing-grade resin (B-PET).

Table III DSC Transition Temperature Change of PET After Recovered or Blended Process

	VB	Flake	Chip	R-PET	R80/E20	R50/E50	R20/E80	E-PET
T_g	86.0	86.2	86.2	82.1	81.4	80.8	78.0	81.4
T_c	193.0	163.0	145.0	143.0	141.0	137.5	141.2	143.0
T_m	248.0	251.0	252.0	254.0	256.4	257.0	258.0	261.5

Temperatures in °C.

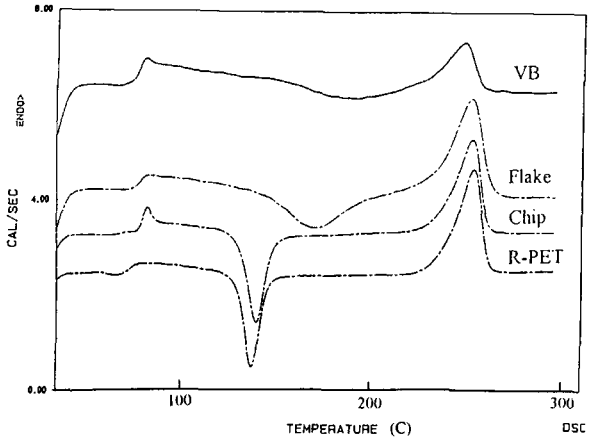

Figure 2 DSC curves of blow-molding PET after recovered process.

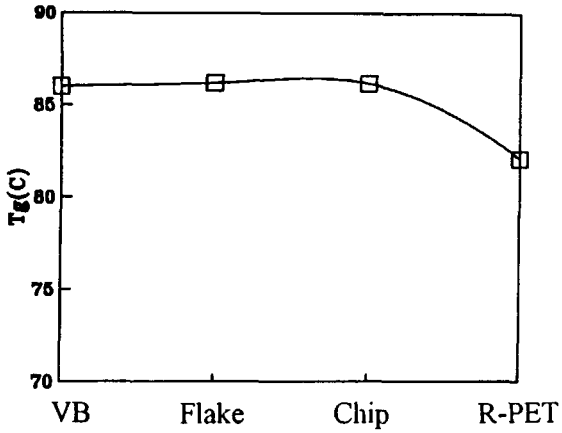

Figure 4 T_g change of blow-molding PET after recovered process.

Mechanical Properties of the R-PET and the Blends

The mechanical properties of tensile and impact strengths and elongations were measured according to the specifications of the ASTM. The results are listed in Table II.

The tensile strength varied from 653 kg/cm^2 of the E-PET to 623 kg/cm^2 of the R-PET. The blends exhibited higher tensile strengths ranging from 5 to 10% increases compared with R-PET or 3 to 5% increases compared with E-PET.

The R-PET has shown a large effect on the elongation properties of the blends. An average of over 10-fold increases of the elongation/stretching strengths better than the E-PET samples was observed. The impact strengths of the blends were also increased, ranging from 3.32 to 4.97 kg-cm/cm, with the minimum increases being threefold better than that of the E-PET (1.1 kg-cm/cm) samples.

In published reports,[14,15] the composition and structures of B-PET and R-PET (recycled B-PET) are quite different from those of E-PET. For the unique application of amorphous appearance, comonomers other than ethylene glycol and terephthalic acid were incorporated, disrupted the regularity of the PET chain, and changed crystallization behavior. Basically, the bottle grade from which R-PET was obtained is more ductile because of lower crystallinity, which persists in the R-PET, compared with E-PET.

It is therefore concluded that R-PET has shown a general trend of positive effect on the mechanical strengths of the E-PET. In any case, all samples containing R-PET in blends show mechanical improvements with large increases on the elongation as well as impact strengths. This is probably due to crystalline morphology and gradients of morphology of the injection-molded samples. For semicrystalline polymers, most mechanical properties depend critically on crystallinity.[16,17] Further evidence of these

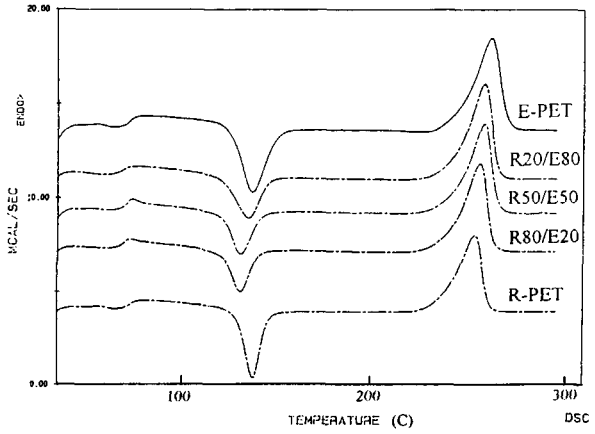

Figure 3 DSC curves of R-/E-PET blends.

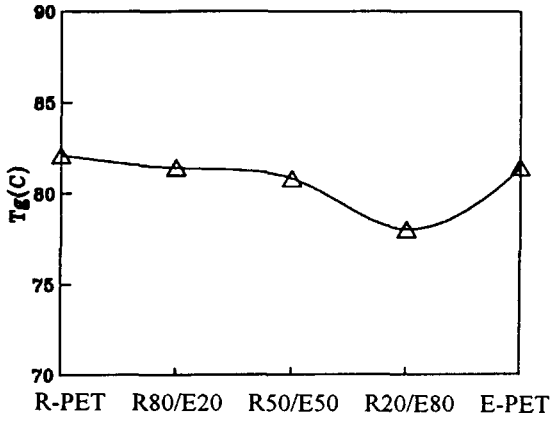

Figure 5 T_g change of R-/E-PET blends.

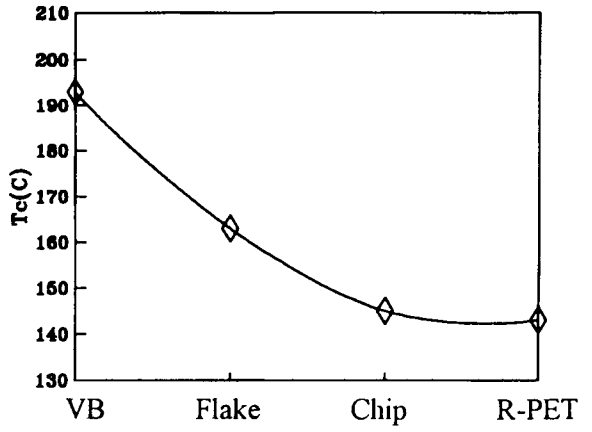

Figure 6 T_c change of blow-molding PET after recovered process.

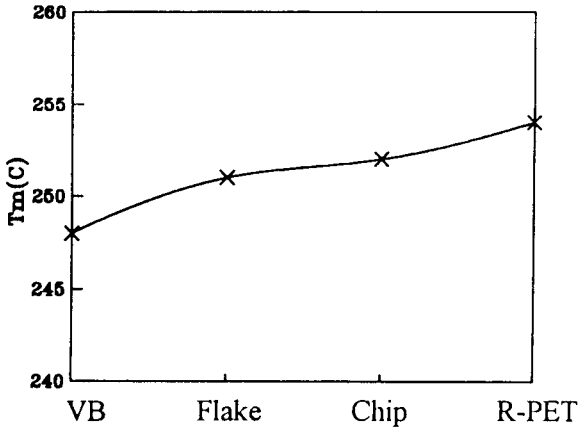

Figure 8 T_m change of blow-molding PET after recovered process.

improved properties will be shown in the crystallinity study by DSC in the following paragraphs and by molecular weight measurements in Part II of this series.

DSC Heating Thermogram

One of the main advantages of thermoplastics is the "reprocessibility" of the materials by a thermal process. The R-PET is subjected to thermal reprocesses, because the applications of PET require this ability for either engineering grade or the recycled materials. Table III shows the measurements of the T_g, T_c, and T_m with the various PET materials of VB (virgin bottle-grade PET resin), flake (crushed PET beverage bottle), chip (extruded pellet), E-PET (injection-molded engineering PET), R-PET (recycled and injection-molded PET), and the R80/E20, R50/E50, and R20/E80 (the blend ratios of R-PET and E-PET in injected blends).

A typical DSC thermogram is shown in Figure 2 in which the VB, flake, chip, and R-PET are shown from the top and down in the diagram as indicated. Figure 3 shows the rest of the E-PET, R20/E80, R50/E50, and R80/E20 samples with the reference of R-PET in descending order from the top to the bottom of the diagram. The thermal properties that are observed are discussed below.

T_g of the PETs

From the DSC thermogram, the T_g, one of the important parameters, is obtained. As one of the second-order thermal transitions, T_g provides information regarding the amorphous portion of a polymer soften.[18] From Figure 4, T_g shows little change for those samples of limited thermal cycles, such as VB, flake, and chip. When subjected to more thermal treatment, the injection-molded sample of R-PET showed the lowering of T_g from 86 to 83°C.

The specimens of R-/E-PET blends show lower T_g values as expected, as shown in Figure 5. This is

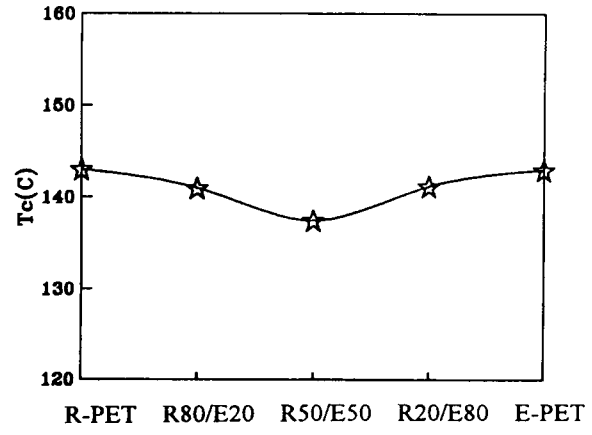

Figure 7 T_c change of R-/E-PET blends.

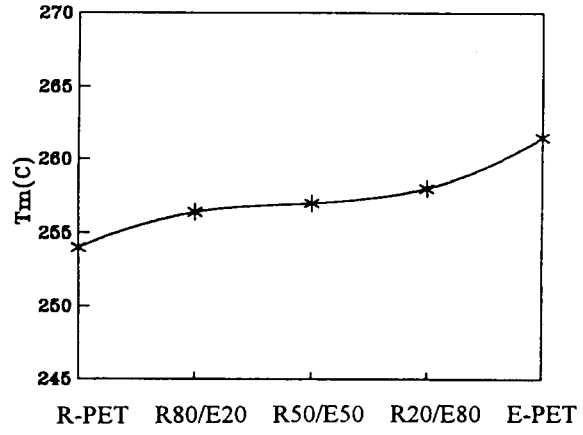

Figure 9 T_m change of R-/E-PET blends.

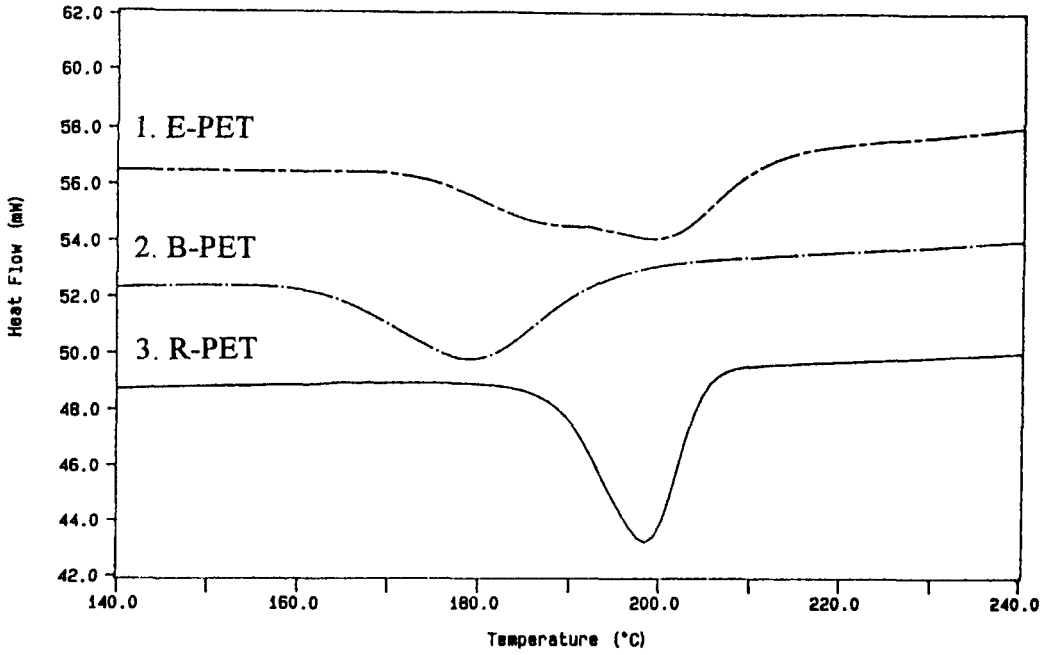

Figure 10 DSC dynamic crystallization curves of single-component PET materials (cooling rate, 10°C/min). (1) E-PET, (2) B-PET, (3) R-PET.

understandable because these blend samples are injection molded. The trend of ease of processing with the increasing thermal cycles for these blends is more pronounced in the measurements of the T_c, where crystallinity begins to appear at that temperature.

The T_c of the PETs

The thermal cycles of the processed samples with their individual T_c values are shown in Figure 6. The changes of the T_c values from samples of virgin resin (VB) to flake to chip and R-PET are very vis-

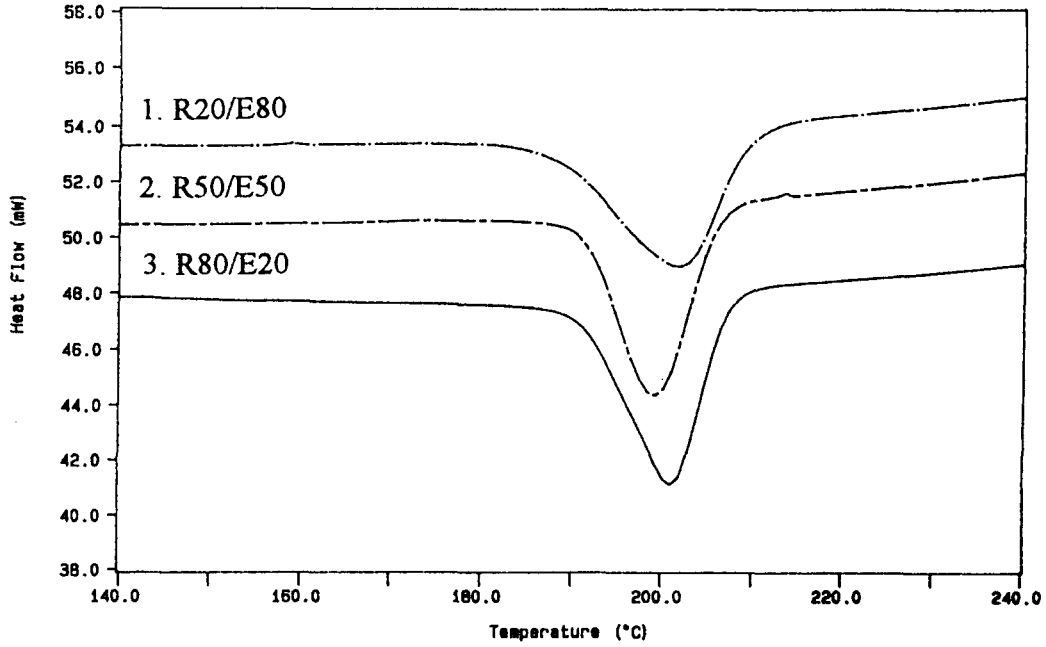

Figure 11 Dynamic crystallization curves of recovered PET blended materials (cooling rate, 10°C/min). (1) R20/E80, (2) R50/E50, (3) R80/E20.

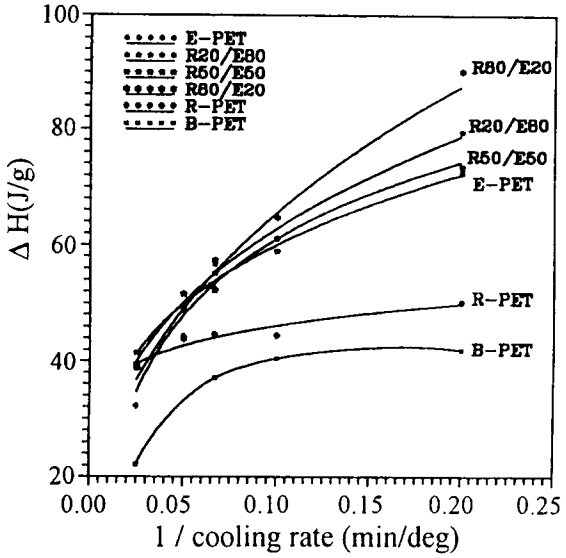

Figure 12 Heat of crystallization as a function of the reciprocal of the cooling rate for various PET samples.

ible and significant. This indication of the lower temperature at which crystallinity begins to appear is quite related to the thermal cycles that the samples endured. Samples with more thermal cycles tend to have a lower T_c, that is, the crystallization of the PET begins at a lower temperature. As one can see from Table III, the T_c values were 193°C for VB and decreased to 163 (flake), 145 (chip), and 143°C for the injection-molded species of R-PET. The decreasing trend is also observed in the blended samples, as shown in Figure 7, with a dip of T_c of 137.5°C for the 50/50 blends of the R-/E-PET samples.

In the DSC heating thermogram study, the significance of the trend is that the threshold above which the crystallization process from the glassy state is beginning to appear and the decreased T_c mean that the R-PET can crystallize more readily than the original or nonthermally cycled samples; in the R-/E-PET blends, once the R-PET is blended, it also can crystallize more readily from the glassy state. In other words, the R-PET and its blends could have more orderly structures in layers. The overall effects of the lower T_c of the R-PET and its blends mean that the PET material of the recycled and blended PET may begin to crystallize from the glassy state at a lower temperature in the heating cycle, which denotes the ease of crystallization. However, the cooling cycle data, which would be more related to the injection-molding process, will be discussed in the next paragraph.

The depressing effect on T_c discussed above is not due to the severe incision of the molecular chains (see molecular weight measurements in Part II of this series) present in the materials. In the case of the chopped backbone of the PET, the mechanical properties of the samples may suffer a setback,[19] not the enhancement as observed. Therefore, the modification of the chain lengths must be limited to the long or too cumbersome segments. This means that the molecule threads protruding from entanglements are attacked first and break off during the thermal recycling process.[20] This thermal cycling process releases the entanglement and increases the crystallinity. With this mild thermal degradation, R-PET is in better condition for the crystallization and the less amorphous segment is retained.

The T_m of the PETs

The measurements of T_m of various PET specimens are shown in Table III. The increasing trend of T_m for samples subjected to various degrees of thermal cycles is shown in Figure 8, and the T_m values of these injection-molded blends are shown in Figure 9. The T_m of VB was 248°C and it increased steadily to 251 (flake), 252 (chip), and 254°C for the injection-molded species of R-PET. T_m is increased after each recovered process. The T_m values for the blended samples are proportional to the T_m values of the blending components: of 254 (R-PET), 256.4 (R80/E20), 257.0 (R50/E50), 258.0 (R20/E80), and 261.5°C (E-PET)

The melting process can be shown by eq. (3):

$$\Delta G = \Delta H - T\Delta S \tag{3}$$

At the melting process, where a steady equilibrium is reached, $\Delta G = 0$ and

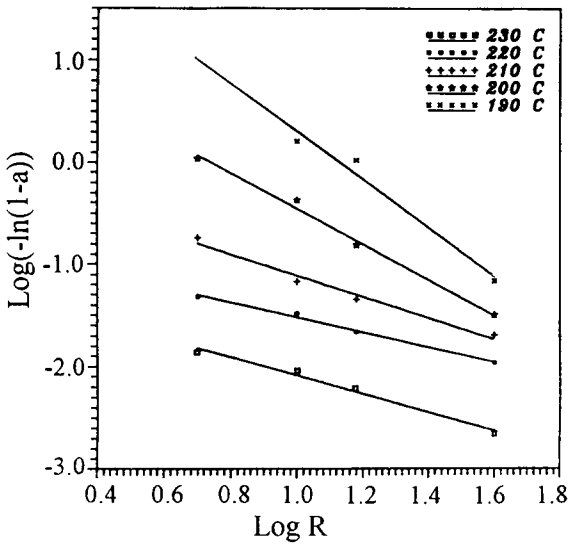

Figure 13 Avrami plot of dynamic crystallization of R50/E50 PET blends at various crystallization temperature.

Table IV Analysis of the Course of Dynamic Crystallization of PET

Temperature (°C)	B-PET		Temperature (°C)	R-PET		E-PET		R80/E20		R50/E50		R20/E80	
	K	*n*		*K*	*n*	*K*	*n*	*K*	*n*	*K*	*n*	*K*	*n*
200	1.16	2.2	230	0.02	0.8	0.08	0.99	0.27	1.55	0.06	0.89	0.07	0.89
190	10.13	2.1	220	0.03	0.6	0.22	0.85	0.93	1.54	0.16	0.72	0.17	0.70
180	67.65	2.0	210	0.19	1.0	1.99	1.33	3.58	1.75	0.82	1.02	0.93	1.02
170	63.60	1.7	200	55.67	2.4	13.67	1.68	85.94	2.50	18.97	1.74	17.62	1.68
160	44.45	1.2	190	95.97	1.9	13.82	1.25	1527	2.78	485.2	2.31	252.9	2.10

For blow-molding virgin PET (B-PET), the cooling crystallization range integrated between 200 and 160°C. The other PETs were integrated between 230 and 190°C.

$$T_m = \Delta H/\Delta S \quad (4)$$

As the crystalline structure becomes more orderly, the entropy, ΔS, the measurement of the disorderliness, is decreased. The T_m is therefore increased.

Concerning the crystallite size, a qualitative analysis can be approached according to Hoffman's nucleation theory,[21-23] where

$$T_m = T_{m^0}[1 - (2\delta e/\Delta Hv \times l)] \quad (5)$$

T_{m^0} is the equilibrium melting point, δe, is the basal interfacial free energy, ΔHv is the heat of fusion of a unit volume of crystal, and l is a thin dimension of crystal.

Because the R-PET is through the recycling process and has the lower T_c threshold temperature, the interfacial free energy of the R-PET could be decreased and the crystalline thickness (l) may be increased as the term of ($2\delta e/\Delta Hv \times l$) becomes smaller. The overall effect may lead the crystalline structure to become thicker with less interfacial free energy. As a result of the thickening effect on the increasing of the crystalline size formation, a more orderly structure and a higher T_m of the R-PET may occur, as measured in the DSC curves in Figures 2 and 8.

The same crystalline behaviors of the R-/E-PET blends with the increasing trend of the T_m values are also shown in Figures 3 and 9. The R- and E-PET blends are crystalline-crystalline isomorphous polymer blends of the same material. Therefore, no melting point depression on mixing or blending is found.[24] The T_m values of the blends are between and proportional to the two starting materials of R-PET and E-PET.

DSC Cooling Thermogram

DSC curves obtained from the cooling cycle of some single-component PET materials are shown in Figure 10, and blends with E-PET are shown in Figure 11. From Figure 10, the B-PET (line 2), the original raw material of a PET bottle, exhibits a rather broad temperature range of crystallization, starting at a lower temperature than either E- (line 1) or R-PETs (line 3). The R-PET shows a higher temperature with a sharper and more narrow temperature range of crystallization than the B-PET or the E-PET. The E-PET also shows a broad peak of crystallization.

On the other hand, all PET samples with R-PET in the blends show various degrees of improvement on the crystallization process. Peaks are in more narrow and sharper shapes than either VB or E-PET, as one can see from the curves in Figure 11.

With the plot of ΔHc, the heat of crystallization, against the reciprocal function of cooling rate, as shown in Figure 12, the amount of crystallinity can be obtained. The R80/E20 PET blend contains the most crystallinity in the slow and medium cooling conditions. All samples containing R-PET have various amounts but higher contents of crystallinities than the three single samples of B-, R-, and E-PETs in the different cooling conditions which dominate the crystalline structures in the injection applications. The most striking feature is the blow-molded original PET with slow crystallization rate and less crystallinity as is needed for that specific application. In addition, Figure 12 shows that E-PET is more crystalline than R-PET, as measured by the heat of crystallization at various cooling rates. It also shows a more transparent, less crystalline surface region for R-PET than E-PET in Figure 1. The higher melting point of the E-PET than the R-PET is listed in Table III. The E-PET probably has larger (higher melting) and more (higher heat of crystallization) crystallites and homogeneity in the injection-molded test specimens than does R-PET. High crystallinity may contribute to rigidity, or

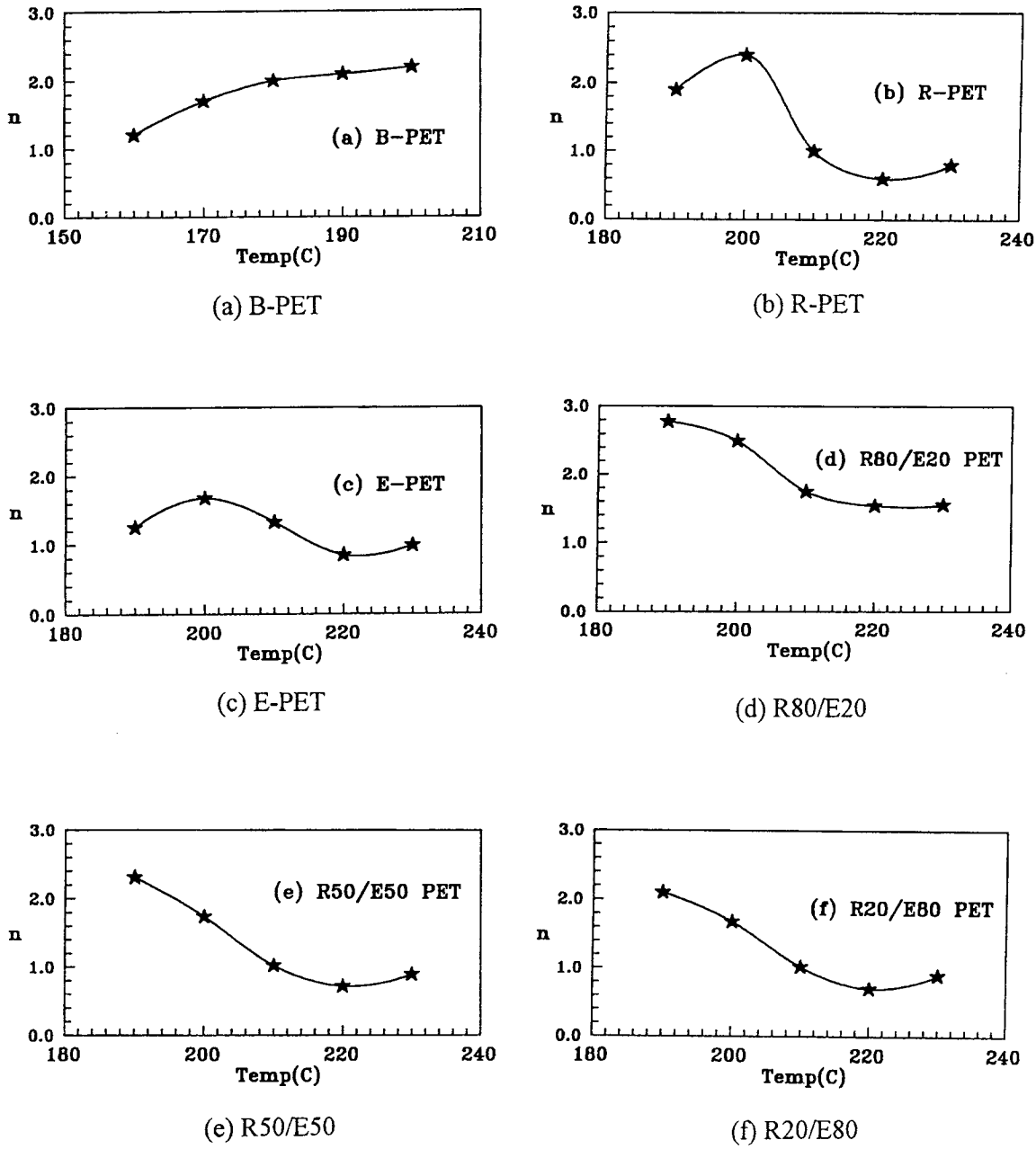

Figure 14 The n values of different PET and PET blends at various cooling temperatures. (a) B-PET, (b) R-PET, (c) E-PET, (d) R80/E20, (e) R50/E50, and (f) R20/E80.

less perfectly, smaller crystallites with a broader size distribution may contribute to elasticity. Injection-molded samples of R-/E-PET blends probably show various levels of morphology and thus show various degrees of improvement on mechanical properties that resulted from the crystallization process. It has also been pointed out[25] that the mechanical properties of injection-molded semicrystalline thermoplastics are probably dependent on the order existing at various levels in the morphology of the polymer.

The Dynamic Crystallization Kinetics

Because different crystallization behaviors were shown in the DSC cooling cycle study, a detailed analysis of the crystallization course was made with the Avrami expression. The crystallization rate constants and the Avrami exponents were calculated. A typical Avrami plot is shown in Figure 13 with the application of the extended Avrami equation for the crystallization of the R50/E50 PET blends. The Avrami exponent n

Table V Values of the Avrami Exponent, for Various Types of Nucleation and Growth[26]

n	Mechanism	Restriction
4	Spherulitic growth from sporadic nuclei	3 dimensions
3	Spherulitic growth from instantaneous nuclei	3 dimensions
3	Disc-like growth from sporadic nuclei	2 dimensions
2	Disc-like growth from instantaneous nuclei	2 dimensions
2	Rod-like growth from sporadic nuclei	1 dimension

was found to be a variant with varying temperature.

The kinetic data of the dynamic crystallization study on these recovered PET and PET blends are listed in Table IV and are shown in Figure 14. These results indicate that the cooling crystallization behavior of B-PET (injected blowing-grade PET) begins at the lowest temperature among all tested samples of 200°C, but after the recovered process (R-PET) or for R-/E-PET blends, the crystallization begins at the higher temperature of 230°C. The E-PET (injected engineering-grade PET) also starts at that 230°C temperature. It also indicates that the rate constant K increases rapidly below 200°C for the B-, E- and R-PETs and more so for all blended samples.

The changes of the Avrami exponent n from high temperature descending to lower temperature for these samples are summarized as follows: B-PET, the (n) change for blow-molding PET between 200 and 160°C is decreasing from 2.2 to 1.8; R-PET, the (n) change for recovered PET between 230 and 190°C has a maximum value of 2.4 at 200°C; E-PET, the (n) change for engineering PET between 230 and 190°C has a maximum value of 1.68 at 200°C; R-80/E20, the (n) change for R-80/E-20 PET between 230 and 190°C is increasing from 1.55 to 2.78; R-50/E50, the (n) change for R-50/E-50 PET between 230 and 190°C is increasing from 0.89 to 2.31; and R-20/E80, the (n) change for R-20/E-80 PET between 230 and 190°C is increasing from 0.89 to 2.1.

In the Avrami expression,[26] the kinetic rate constant K is a function of nucleation and the growth rate. The Avrami exponent provides qualitative information on the nature of nucleation and the growth processes. The various values and elucidation which can be obtained for n are listed in Table V.

From the Avrami exponent n analysis, a higher order structure was found in the blends of R80/E20, R50/E50, and R20/E80, especially in the R80/E20 blends. The Avrami equation provides useful data on the overall kinetics of crystallization. In addition, the model of Keith and Padden on spherulitic crystallization[27-30] can be used to interpret the n value's variation for different PET compositions.

For the kinetics of spherulitic crystallization, eq. (6) is indicated where $\delta = D/G$ δ is the quantity, a dimension of length, that determines the lateral dimensions of the lamellae, D is the diffusion coefficient for impurity in the melt, and G is the radial growth rate of a spherulite. By logarithmic differentiation of $\delta = D/G$, eq. (6) is obtained.

$$1/\delta(d\delta/dT) = 1/D(dD/dT) - 1/G(dG/dT) \quad (6)$$

The derivative dD/dT always has a positive value, and dG/dT may be positive or negative.

The coarseness of the spherulites depends on which of the two terms on the right of eq. (6) is the larger. If the quantity on the right-hand side of the equation is positive, an increase in coarseness is expected as the temperature is increased.

The radial growth rate, G, may be described by eq. (7).

$$G = G^0 e^{\Delta E/RT} e^{-\Delta F^*/RT} \quad (7)$$

where ΔF^* is the free energy of formation of a surface nucleus of critical size, and ΔE is the free energy of activation for a chain crossing the barrier to the crystal. Equation (7) allows the temperature dependence of spherulite growth rates to be understood in terms of two competing processes. Opposing one another are the rates of two competing processes of nucleation and molecular mobility (molecular transport). Molecular transport in the melt increases with increasing temperature, and the rate of nucleation decreases with increasing temperature. According to Keith and Padden,[27] diffusion is the controlling factor at low temperatures, whereas at higher temperatures, the rate of nucleation dominates. Between these two extremes, the growth rate passes through a maximum where the two factors are approximately equal in magnitude. R-PET and E-PET follow this model, and the maximum n values were found at 200°C, as shown in Figure 14(b) and (c). For the R-/E-PET blends, however, the molecular

mobility is increased, as is discussed in the above paragraph. When temperature changes from high temperature descending to low temperature, the component ΔE (the free energy of activation for a chain crossing the barrier to the crystal), which is the low temperature-controlling factor, is getting less effective and less influential, so the compromised even point was broken, and no maximum point of growth rate was formed in this temperature range. Instead, a monotonous increasing trend of n with temperature decreasing was found, as shown in Figure 14(d) through (f). For B-PET, the blow molding-grade materials, amorphous in nature for its specific application, the n value is decreasing with temperature descending. With the cumbersome molecule, diffusion is the controlling factor at low temperature, as shown in Figure 14(a).

CONCLUSIONS

Dynamic cooling crystallization is one of the versatile tools of the DSC for the study of crystallization and can be used to detect the individual crystalline behavior of the material. The study of the thermal properties may provide an understanding related to the mechanical properties, as shown in R-PETs. The enhanced mechanical properties of the R-PET are explained as the result of the various levels in crystallinity of the R-PET. The thermal cycle of the PET proves to be an important factor, and the variable crystallization exponent (n) of the Avrami equation is detected in these PET materials.

REFERENCES

1. W. H. Cobbs and R. L. Burton, *J. Polym. Sci.*, **10,** 275 (1953).
2. A. Keller, G. R. Lester, and C. B. Morgan, *Philos. Trans. R. Soc. Lond.*, **A247,** 1 (1954).
3. F. D. Hartly, F. W. Lord, and L. B. Morgan, *Philos. Trans. R. Soc. Lond.*, **A247,** 23 (1954).
4. J. B. Jackson and G. W. Longman, *Polymer,* **10,** 873 (1969).
5. F. Van Antwerpen and D. W. Van Krevelen, *J. Polym. Sci. Polym. Phys.*, **10,** 2423 (1972).
6. R. Tant and W. T. Culberson, *Polym. Eng. Sci.*, **33,** 1152 (1993).
7. J. D. Hoffman, *J. Chem. Phys.*, **28,** 1192 (1958).
8. V. G. Baranov, A. V. Kenarov, and T. I. Volkov, *J. Polym. Sci.*, C, **30,** 271 (1970).
9. S. A. Jabarin, *J. Appl. Polym. Sci.*, **34,** 85 (1987).
10. S. A. Jabarin, *J. Appl. Polym. Sci.*, **34,** 97 (1987).
11. D. M. Fann, J. S. Chow, S. K. Huang, and J. J. Lee, *Proc. 16th ROC Polym. Symp.*, **2,** 149, (1993).
12. J. S. Chow, D. M. Fann, S. K. Huang, and J. J. Lee, *Proc. 16th ROC Polym. Symp.*, **1,** 271 (1993).
13. T. Ozawa, *Polymer,* **12,** 150 (1971).
14. P. A. Aspy and E. E. Denison, *Mod. Plastics,* **August,** 74 (1983).
15. D. V. Rosato and D. V. Rosato, *Blow Molding Handbook,* Hanser Publisher, New York, 1989, Chap. 14.
16. N. G. McCrum, C. P. Buckley, and C. B. Bucknall, *Principles of Polymer Engineering,* Oxford University Press, New York, 1988, Chap. 2.
17. F. A. Bovey and F. H. Winslow, *Macromolecules: An Introduction to Polymer Science,* Academic Press, New York, 1979, Chap. 6.
18. L. H. Sperling, *Introduction to Physical Polymer Science,* Wiley, New York, 1992, Chap. 1.
19. K. Chrien and J. Reyes, *Eng. Plastics,* **4,** 262 (1993).
20. G. Menges, *Int. Polym. Sci. Tech.*, **20,** T/20 (1993).
21. J. D. Hoffman, *Polymer,* **24,** 3 (1983).
22. J. D. Hoffman, *Polymer,* **23,** 656 (1982).
23. E. A. Dimarzio, C. M. Guttman, and J. D. Hoffman, *Faraday Discuss. Chem. Soc.*, **68,** 210 (1979).
24. P. J. Flory, *Principles of Polymer Chemistry,* Cornell University Press, Ithaca, NY, 1953, Chap. 8.
25. A. Sharples, *Introduction to Polymer Crystallization,* Edward Arnold (Publishers), London, 1966, Chap. 10.
26. A. Sharples, *Introduction to Polymer Crystallization,* Edward Arnold (Publishers), London, 1966, Chap. 4.
27. H. D. Keith and F. J. Padden, Jr., *J. Appl. Physiol.*, **35,** 1270 (1964).
28. H. D. Keith and F. J. Padden, Jr., *J. Appl. Physiol.*, **35,** 1286 (1964).
29. H. D. Keith and F. J. Padden, Jr., *J. Appl. Physiol.*, **34,** 2409 (1963).
30. L. H. Sperling, *Introduction to Physical Polymer Science,* Wiley, New York, 1992. Chap. 6.